

Giant Dielectric Permittivity of Electron-Doped Manganite Thin Films, $\text{Ca}_{1-x}\text{La}_x\text{MnO}_3$ ($0 < x < 0.03$)

J. L. Cohn and M. Peterca^y

Department of Physics, University of Miami, Coral Gables, Florida 33124

J. J. Neumeier

Department of Physics, Montana State University, Bozeman, Montana 59717

A giant low-frequency, in-plane dielectric constant, $\sim 10^6$, for epitaxial thin films of $\text{Ca}_{1-x}\text{La}_x\text{MnO}_3$ ($x < 0.03$) was observed over a broad temperature range, 4K $< T < 300$ K. This phenomenon is attributed to an internal barrier-layer capacitor (IBLC) structure, with Schottky contacts between semiconducting grains. The room-temperature permittivity increases substantially with electron (La) doping, consistent with a simple model for IBLCs. The measured values of ϵ' exceed those of conventional two-phase IBLC materials based on $(\text{Ba,Sr})\text{TiO}_3$ as well as recently discovered $\text{CaCu}_3\text{Ti}_4\text{O}_{12}$ and (Li,Ti) -doped NiO .

PACS numbers: 77.22.Ch, 77.22.Gm, 77.55.+f, 77.84.Bw

I. INTRODUCTION

High-permittivity dielectric materials play an important role in electroceramic devices such as capacitors and memories. Recent reports of giant permittivity have directed considerable attention to several new material systems: non-ferroelectric $\text{CaCu}_3\text{Ti}_4\text{O}_{12}$,¹ percolative BaTiO_3 -Ni composites,² and (Li,Ti) -doped NiO .³ Of particular interest for applications is the weakly temperature dependent permittivity of these materials near room temperature. The enormous dielectric constant of these materials, $\sim 10^6$, appears to be⁴ a consequence of an internal barrier-layer capacitor (IBLC) structure, composed of insulating layers between semiconducting grains. IBLCs with effective $\epsilon' \sim 10^6$ based on $(\text{Ba,Sr})\text{TiO}_3$ are well known,⁵ but their usefulness is limited by a strong frequency and temperature dependence of their dielectric constant. Thus the newly discovered materials suggest that increases in values and/or simplification of processing could yield new and useful IBLC materials.

Here we report on giant values of the effective dielectric constant, $\sim 10^6$, observed at low frequencies ($f < 100$ kHz) for thin films of the electron-doped manganite, $\text{Ca}_{1-x}\text{La}_x\text{MnO}_3$ ($0 < x < 0.03$). The large and weakly T - and f -dependent near room temperature is attributed to an IBLC microstructure, comprising a network of depletion layers between semiconducting grains.

is enhanced by electron doping via La substitution for Ca or oxygen reduction.

II. EXPERIMENTAL METHODS

Polycrystalline targets of $\text{Ca}_{1-x}\text{La}_x\text{MnO}_3$ ($x < 0.03$) were prepared by solid-state reaction as described previously.⁶ Powder x-ray diffraction revealed no secondary phases and iodometric titration, to measure the average Mn valance, indicated an oxygen content for all targets within the range 3.00 \pm 0.01. Thin films were

grown by pulsed laser deposition using a 248 nm KrF excimer laser, with energy density 0.8 ± 0.2 J/cm², pulse repetition rate 10 Hz, and target-substrate distance, 4 cm. The films were deposited on LaAlO_3 (LAO) substrates of [100] orientation, with substrate temperature 750 \pm 50 C and oxygen pressure 200 mTorr. Following the depositions, the chamber was filled to 700 Torr oxygen, held at 500 C for 30 min., and subsequently cooled to room temperature. Film thicknesses were 50–170 nm. X-ray diffraction (XRD) indicated epitaxial growth of the pseudocubic perovskite for all films, with lattice parameter, $a = 3.72$ Å for CaMnO_3 . The full widths at half maximum of the (200) film reflections were typically 0.4 $^\circ$. Scanning electron microscopy indicated an average grain size of 0.5–1 μ m. Impedance measurements were performed with a Hewlett-Packard model 4263B LCR meter in the frequency range 100 Hz to 100 kHz. A model HP16034E test fixture was used at room temperature, and a coaxial-lead, four-terminal pair arrangement in a cryostat for low temperatures. Silver paint electrodes, annealed at 300 C, were applied on opposing edges of the specimens so that the ac voltage (0.2 V for all measurements) was applied in the film plane. In this configuration, the film and substrate capacitances are additive; the equivalent circuit for contacts, film and substrate is shown in the inset of Fig. 1. A contact capacitance can lead to apparently large values⁸ of ϵ' and thus great care is required to distinguish the true response of the sample. To address this issue, contact contributions to the impedance were eliminated at room temperature for some films by measuring the length dependence of the impedance ($Z_{\text{film}} + Z_{\text{substrate}}$), $Z = R + jX$, on a series of films deposited simultaneously onto pre-cut substrates of different length, l . Since the contact capacitance and resistance should be independent of l , the measured reactance and resistance should be linear in l , $X = X_0 - l$ and $R = R_0 + l$, respectively. $X_0 = -l / R_C^2 C_C = [1 + (l / R_C C_C)^2]$ is a constant determined by a small serial inductance, L (also assumed

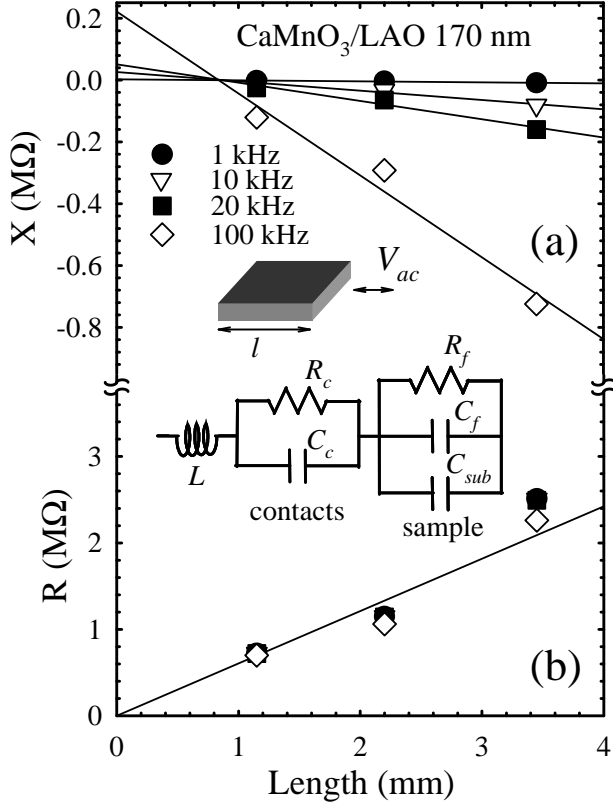


FIG. 1: (a) $X(l)$ and (b) $R(l)$ for a 170-nm $\text{CaMnO}_3/\text{LAO}$ film at room temperature. The inset shows the contact configuration and equivalent circuit.

independent of l),⁹ and the capacitive reactance of the contacts. These relations are followed well by the raw data (Fig. 1). The dielectric constant of the film was computed as,

$$\epsilon_f = \frac{1}{\epsilon_0 A_f} \frac{A_{\text{sub}}}{2 + 0.2} \quad (1)$$

where $\omega = 2\pi f$ is the angular frequency of the applied voltage, A_f (A_{sub}) is the film (substrate) contact area and ϵ_{sub} is the substrate dielectric constant. The latter, determined from a similar analysis of $Z(l)$ for blank substrates, was $\epsilon_{\text{sub}} = 24$ in good agreement with published values.¹⁰ Uncertainty in ϵ_f determined from Eq. (1), arising principally from scatter in the data, was typically

20%. Values for ϵ_f determined from the length dependence analysis were consistently larger than those determined from direct measurements, indicating a predominance of the inductive reactance over the capacitive reactance of the contacts (i.e. $X_0 > 0$). The $\epsilon(T)$ data presented below from direct measurements thus underestimate the true magnitude. The uncertainty in ϵ_f for the direct measurements near room temperature (where $C_f \approx C_{\text{sub}}$) is given by that of the film thickness ($\sim 10\%$). At the lowest temperatures, where $C_f \ll C_{\text{sub}}$, the uncertainty in ϵ_f is 50%, largely due to a 5% uncertainty

in C_{sub} . For all measurements, the impedance was independent of ac voltage (50 mV–1 V) and applied DC bias (0–2 V).

III. RESULTS AND DISCUSSION

The impedance of the target materials was measured in separate experiments. CaMnO_3 is an antiferromagnetic ($T_N = 125\text{ K}$) semiconductor with a small electron density associated with native defects, particularly oxygen vacancies, that yield a substantial room temperature conductivity, $\sim 100^{-1} \text{ m}^{-1}$. Electron doping via La substitution for Ca further enhances, especially at low T .⁶

could be determined reliably only at $T < 100\text{ K}$ where the capacitive reactance was sufficiently large (> 0.1). It was describable as a sum of a constant term $\sim 25-50$ (the high-frequency and lattice terms) and a dipolar contribution associated with hopping charge carriers.⁷ The latter gives rise to steps in $\epsilon(T)$ which occur at lower T with decreasing frequency, as shown for CaMnO_3 in Fig. 2 (a) (solid curves). This indicates a relaxation process associated with thermal activation of localized charge carriers, characterized by a relaxation time, $\tau = \tau_0 \exp(U/k_B T)$. Analyzing the maxima in $d\epsilon/dT$ (corresponding to $\omega\tau = 1$) we find $U = 103\text{ meV}$ and $\tau_0 = 7.5 \times 10^{-14}\text{ s}$. These parameters are typical of polaronic relaxation in LaMnO_3 ¹¹ and other perovskites.¹² For comparison, $U = 54\text{ meV}$, $\tau_0 = 8.4 \times 10^{-10}\text{ s}$ were reported for single-crystal $\text{CaCu}_3\text{Ti}_2\text{O}_{12}$,¹³ and $U = 313\text{ meV}$, $\tau_0 = 8.5 \times 10^{-13}\text{ s}$ for (Li,Ti)-doped NiO .³ Relevant to the subsequent discussion of films, it was found that increasing the electron density, either through oxygen reduction or La doping, resulted in a decrease (increase) in U (τ_0). Further details of measurements on the polycrystalline bulk materials will be presented elsewhere.¹⁴

Figure 2 (a) shows $\epsilon(T)$ at three frequencies ($\sim 20\text{ kHz}$) for a 170-nm film of CaMnO_3 . The inset shows $\epsilon(T)$ at room temperature for a second piece of the same film measured to 100 kHz. At low temperatures, ϵ has a magnitude comparable to the bulk material and small steps occur at temperatures similar to those at which the bulk material exhibits dipolar relaxation. With increasing temperature a second dispersive step is observed near 200 K, with ϵ increasing by an order of magnitude. For $T > 200\text{ K}$, $\epsilon \sim 3-4 \times 10^4$ with weak temperature and frequency dependencies. Both steps in ϵ appear as maxima in the dielectric loss [$\tan \delta$, Fig. 2 (b)]. The appearance of the high-temperature step is typical of IBLC materials where insulating barriers separate semiconducting grain interiors. Such a system can be modelled as two RC circuits in series, one for the grain interiors and one for the grain-boundary response.⁴ The grain-boundary RC time constant, $\tau = R_{\text{gb}}C_{\text{gb}}$, gives rise to a second relaxation process that is thermally activated via the behavior of R_{gb} . From the temperatures of the maxima in $\tan \delta$ measured for two pieces of this film we compute [inset, Fig. 2 (b)] average values for activation energies

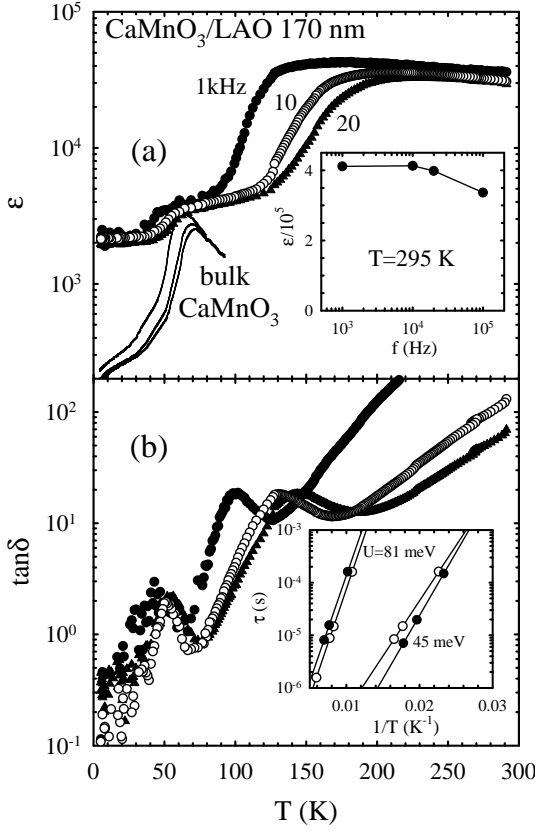


FIG. 2: (a) $\epsilon(T)$ and (b) $\tan \delta(T)$ at three frequencies for a 170-nm $\text{CaMnO}_3/\text{LAO}$ film. The solid curves in (a) are for bulk CaMnO_3 at the same frequencies. The inset in (a) shows ϵ at room temperature for a second piece of the same film. The inset in (b) shows Arrhenius behavior of relaxation times determined from peaks in $\tan \delta$ for both pieces of the film and corresponding average activation energies.

$U = 45 \pm 6$ [81 ± 2] meV and $\tau_0 = (1.6 \pm 1.2) \times 10^{-9}$ s [(9.4 $\pm 3.5) \times 10^{-9}$ s] for the grain interior [grain-boundary] relaxations. The values of U and τ_0 inferred for the grain interiors are significantly smaller and larger, respectively, than the corresponding values determined for the targets. This indicates that the grains of the film are more oxygen deficient, and suggests oxygen is lost during deposition. Consistent with this conclusion, the films have¹⁴ $T_N \approx 200$ K in accord with magnetic measurements on oxygen deficient, bulk CaMnO_3 .¹⁵ Figure 3 shows $\epsilon(T)$ and $\tan \delta(T)$ for a 55-nm film grown from a $\text{Ca}_{0.97}\text{La}_{0.03}\text{MnO}_3$ target. The qualitative features of the data for the as-prepared specimen (open symbols) are similar to that of the CaMnO_3 film except that ϵ is substantially larger, $\approx 10^6$ at 300 K and the lower temperature step in ϵ is absent. The higher carrier density of the La-doped material suppresses the carrier freeze-out responsible for the low- T relaxation to temperatures below our measurement range.¹⁴ A greater dc conductivity is responsible for the sharp increase of $\tan \delta$ at higher temperatures. The grain-boundary relaxation is evident

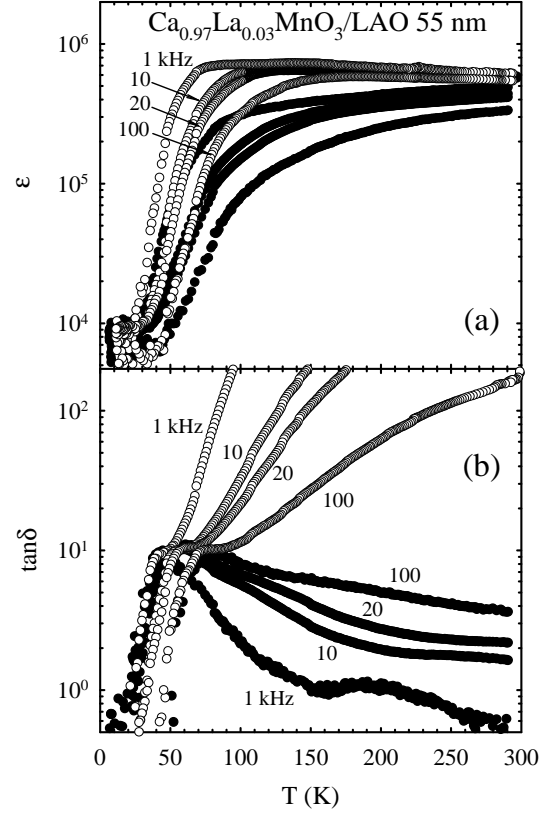


FIG. 3: (a) $\epsilon(T)$ and (b) $\tan \delta(T)$ at several frequencies for a 55-nm $\text{Ca}_{0.97}\text{La}_{0.03}\text{MnO}_3/\text{LAO}$ film, as-prepared (open symbols) and "aged" for 3 months in air at room temperature (closed symbols).

as weak maxima or plateaus in $\tan \delta$. Analysis of the relaxation yields, $U = 32$ meV and $\tau_0 = 1.1 \times 10^{-8}$ s. After sitting in ambient conditions for three months, ϵ at 300 K for the same specimen (solid symbols) decreased by 20–30%, but $\tan \delta$ had decreased dramatically; by more than four orders of magnitude at 1 kHz and nearly two orders of magnitude at 100 kHz (Fig. 3). At lower temperatures, $\tan \delta$ exhibits well-defined maxima, and below these maxima matches the data in the as-prepared state. Thus much of the loss near room temperature in the as-prepared film is associated with dc conduction that is substantially suppressed with "aging".

As for other IBLCs composed of compound semiconductor, our data can be understood by considering the film to be random arrays of close-packed, electrically-active semiconducting grains. Boundaries between grains contain an interface charge Q_i , and are adequately described as double Schottky barriers¹⁶ with capacitance, $C_{\text{DSB}} = \epsilon_0 A / 2x_0$, where A is the area of contact between grains, ϵ is the bulk semiconductor dielectric constant, $x_0 = Q_i / 2N_0$ is the depletion layer width on either side of the grain boundary (assumed symmetric), and N_0 is the donor density in the bulk semiconducting

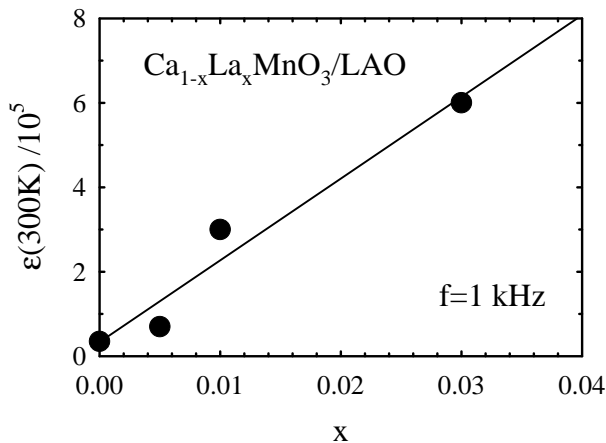


FIG. 4: Doping dependence of the room temperature dielectric constant at 1 kHz.

grains. Since the grain diameter D is typically $\sim x_0$, the "brickwork" model⁵ can be applied to the array of grains, such that the effective dielectric constant is given approximately as, $\epsilon_{eff}(D=2x_0) = DN_0 = Q_i$.

With increased electron (La) doping, ϵ_{eff} for the films increases considerably (Fig. 4). This data allows for a test of the simple model above. Reasonably assuming that the oxygen vacancy concentration (y) for the films is independent of x , we compute the slope, $d\epsilon_{eff}/dx$, by making the substitution $N_0 = (x + 2y)/V_{fu}$,

$$\frac{d\epsilon_{eff}}{dx} = \frac{D}{Q_i V_{fu}} \quad (2)$$

where $V_{fu} = 51 \text{ \AA}^3$ is the volume per formula unit.¹⁷ The line in Fig. 4 yields $d\epsilon_{eff}/dx \approx 2 \times 10^5$. Using 10^5 (Fig. 2 and Ref. 14) and $D = 0.5 \text{ \mu m}$ (from scanning electron microscopy), we compute an interface charge density of $Q_i \approx 5 \times 10^{-7} \text{ m}^{-2}$. This value is typical of those found for a variety of compound semiconductors.¹⁶ That ϵ_{eff} is approximately linear in x implies that variations in ϵ_{eff} and Q_i with doping are either negligible or cancel.

The aging effect in the films is most likely associated with oxidation at grain surfaces. This hypothesis is sup-

ported by preliminary oxygen annealing studies on a 55 nm CMO film. $\tan \delta$ was reduced by a factor of two with no measurable change in ϵ_{eff} following a 15-hour, low-oxygen anneal at 700 °C. A small decrease in ϵ_{eff} for aged films is consistent with a small increase in Q_i .

Finally, we note that the large values of ϵ_{eff} reported here are not limited to manganite films with compositions near 100% Ca. We have measured $\epsilon_{eff} \approx 10^5$ at room temperature for a 55 nm film grown under identical conditions from a $\text{La}_{0.7}\text{Ca}_{0.3}\text{MnO}_3$ target (a colossal magnetoresistance composition). Films of other insulating compositions with the appropriate microstructure may also possess a large effective ϵ_{eff} .

IV. CONCLUSIONS

In summary, thin films of $\text{Ca}_{1-x}\text{La}_x\text{MnO}_3$ ($0 < x < 0.03$) have been found to exhibit giant low-frequency dielectric constants, $\epsilon_{eff} \approx 10^5$, that are weakly temperature and frequency dependent near room temperature. These enormous values are attributed to a barrier-layer capacitor microstructure produced during deposition and subsequent exposure to air by oxidation of grain boundary regions which form an insulating shell on semiconducting grains. ϵ_{eff} increases with charge-carrier doping, consistent with a reduction in the depletion-layer width at grain boundary contacts and a nearly doping-independent surface charge. Though lower dielectric losses will be required for applications ($\tan \delta \approx 0.05$ is desirable), the considerable reduction of $\tan \delta$ upon aging or oxygen annealing with little decrease in ϵ_{eff} motivates further investigations of processing conditions.

ACKNOWLEDGMENTS

The authors gratefully acknowledge experimental assistance from Dr. B. Zawilski. The work at the Univ. of Miami was supported, in part, by NSF Grant No.'s DMR-9504213 and DMR-0072276, and at Montana State Univ. by Grant No. DMR-0301166.

^y present address: Physics Department, University of Pennsylvania, Philadelphia, PA

¹ M. A. Subramanian et al., J. Solid St. Chem. 151, 232 (2000); A. P. Ramirez et al., Sol. St. Commun. 115, 217 (2000).

² C. Pecharron et al., Adv. Mater. 13, 1541 (2001).

³ J. Wu et al., Phys. Rev. Lett. 89, 217601 (2002).

⁴ D. C. Sinclair et al., Appl. Phys. Lett. 80, 2153 (2002).

⁵ C. F. Yang, Jpn. J. Appl. Phys. 36, 188 (1997).

⁶ J. J. Neumeier and J. L. Cohn, Phys. Rev. B 61, 14319 (2000).

⁷ A. K. Jonscher, Dielectric Relaxation in Solids, (Chelsea Dielectrics Press, London, 1983).

⁸ P. Lunkenheimer et al., Phys. Rev. B 66, 052105 (2002).

⁹ Any inductance from the film would be expected to scale with l , tending to reduce the value of ϵ_{eff} in Eq. (1); since ϵ_{eff} is the computed dielectric constant represents a lower bound.

¹⁰ see, e.g., Handbook of Thin Film Devices, ed. by M. H. Francombe, (Academic, New York, 2000), Vol. 3, Ch. 1, p. 19.

¹¹ A. Seeger et al., J. Phys. Cond. Mat. 11, 3273 (1999).

¹² O. Bidault et al., Phys. Rev. B 52, 4191 (1995).

¹³ C. C. Homes et al., Science 293, 673 (2001).

¹⁴ J. L. Cohn, M. P. Peterca, and J. J. Neumeier, Phys. Rev. B, in press (cond-mat/0410657).

¹⁵ J. Bratko et al. Phys. Rev. B 53, 14020 (1996).

¹⁶ F. Greuter and G. Blatter, Semicond. Sci. Technol. 5, 111 (1990).

¹⁷ C. D. Ling et al., Phys. Rev. B 68, 134439/1-8 (2003).